



Surface reconstruction of clean bcc-Fe{1 1 0}: A quasi-hexagonal top-layer with periodic height modulation

T.K. Yamada *, H. Tamura, M. Shishido, T. Irisawa, T. Mizoguchi

Faculty of Science, Gakushuin University, 171-8588 Mejiro, Tokyo, Japan

ARTICLE INFO

Article history:

Received 14 October 2008

Accepted for publication 18 November 2008

Available online 27 November 2008

Keywords:

Surface relaxation and reconstruction

Iron

Whiskers

Single crystal surfaces

Magnetic surfaces

Phase transition

Surface structure, morphology, roughness, and topography

Scanning tunneling microscopy

ABSTRACT

Hexagonal-pillar shaped pure Fe single crystal whiskers with six {1 1 0} side planes were obtained by means of chemical vapor deposition. Atomically resolved scanning tunneling microscopy images obtained on the {1 1 0} surface showed a quasi-hexagonal atomic array with mesoscopic-range periodic height modulation of about 1/3 of an atomic step. This height modulation was found to be a result of an interference between the quasi-hexagonal top-layer and the sub-surface bcc-Fe{1 1 0} layer. Unit vectors of the mesoscopic-range modulation turned out to be expressed as $\begin{pmatrix} \vec{p}_1 \\ \vec{p}_2 \end{pmatrix} = \begin{pmatrix} 13 & 1 \\ -2 & 14 \end{pmatrix} \begin{pmatrix} \vec{u}_1 \\ \vec{u}_2 \end{pmatrix} = \begin{pmatrix} 12 & 1 \\ -3 & 15 \end{pmatrix} \begin{pmatrix} \vec{s}_1 \\ \vec{s}_2 \end{pmatrix}$, where $\begin{pmatrix} \vec{u}_1 \\ \vec{u}_2 \end{pmatrix}$ and $\begin{pmatrix} \vec{s}_1 \\ \vec{s}_2 \end{pmatrix}$ are the primitive vectors of the two-dimensional atomic array in the top-layer and those in the sub-surface layer, respectively. The two-dimensional density of atoms in the top-layer is slightly higher by 0.46% than that in the sub-surface layer.

© 2008 Elsevier B.V. All rights reserved.

1. Introduction

Iron is an important popular ferromagnetic metal which has been widely used since the ancient age in practical applications owing to its strength and abundance. It is a typical bcc-metal at room temperature, however, it takes fcc γ -phase 1185–1667 K and bcc δ -phase (1667–1811 K: melting point) at 1 atm [1], suggesting that the free energy depends delicately on the crystal structure [2]. In a bcc crystal each atom has 8 nearest and 6 second nearest neighbors (NN) in bulk, while an atom at the surface has reduced coordination, i.e. 4 NN and 5 second NN for {001} and 6 NN and 4 second NN for {110}. In general, a break down of the symmetry of atomic interactions generates stress, which causes surface reconstruction in the case that the stress exceeds the elastic limit. There have been found several surface reconstructions on metal surfaces ([3] and references therein). There are three types of them; (1) surface atoms move parallel to the surface to form a larger unit cell, e.g. W{001}-c(2 × 2) [4]. (2) A top surface atomic layer of noble metals forms a hexagonal lattice, e.g. Au{001}-(5 × 20), Pt{001}-(5 × 20), Ir{001}-(5 × 1) [3,5]. (3) Periodic missing atomic rows are formed on the surface, e.g. Pt{1 1 0}-(1 × 2) [6].

Since impurities on metal single crystal surfaces induce surface reconstruction [7,8], one must pay a lot of attention whether the surface reconstruction is of surface intrinsic origin. Adsorbates of the impurities induce reconstruction on Fe surfaces [7,8]. So-called Fe single crystals which were made by a strain-anneal method include several impurities, such as C, P, and S in bulk. These segregate on the surface after every sample-annealing process and cover the Fe surface. Therefore, for a study of clean Fe surfaces, bcc α -Fe{001} single crystals made by a chemical vapor deposition (CVD) technique, which are called Fe-whisker single crystals, have been used since the whiskers consist of only Fe in bulk [9–13]. Although many investigations have been made on clean pure bcc-Fe-whisker single crystals, so far no surface reconstruction has been reported on {001} surfaces.

There have been plenty of investigations on Fe films of different modifications grown epitaxially on single crystal substrates, e.g. W, GaAs, Cu, or Au [14–18]. These Fe films suffer large stress caused by lattice mismatch between the Fe films and the substrate, and the surfaces are frequently reconstructed.

In this study, we discovered a new surface reconstruction on clean bcc-Fe{1 1 0} surfaces of three different pure hexagonal-pillar shaped α -Fe-whisker single crystals. The top surface layer is reconstructed to a quasi-hexagonal lattice with periodic height modulation in mesoscopic-range due to the interactions with the sub-surface bcc-{1 1 0} layer.

* Corresponding author. Tel.: +49 721 608 3441; fax: +49 721 608 6103.
E-mail address: bb96@pi.uni-karlsruhe.de (T.K. Yamada).

2. Experimental

CVD has been used in order to get bcc α -phase Fe single crystals. From the gas phase, extremely high quality Fe-whiskers can be grown [9–13]. Most of the produced whiskers were rectangular pillar shape with six {001} surfaces [10]. We found, however, that a very few crystals had a hexagonal prism shape as shown in Fig. 1a. Laue X-ray diffraction patterns (Fig. 1b) and four-circle X-ray diffraction data (Fig. 1c–h) show that these whiskers grow along $\langle 111 \rangle$ direction with six side planes of bcc- $\{110\}$ surfaces.

Contaminations on the Fe-whiskers were investigated by Auger spectroscopy and scanning tunneling microscopy (STM) in ultra-high vacuum (UHV). Before cleaning, the Fe-whisker was covered by oxide layers. The whisker was cleaned by Ar ion sputtering at 600 °C in a preparation chamber by following the procedure described in Ref. [12]. After these treatments, Auger spectra showed no oxygen. The clean Fe-whisker of hexagonal-pillar shape (Fig. 1a) was mounted in our STM chamber ($<1 \times 10^{-8}$ Pa). A W tip, which was cleaned by Ar ion sputtering and electron bombardment, approached the side plane of the whisker. All STM measurements were performed at room temperature (RT), and the STM images were obtained at negative bias voltages to obtain topography of sample surfaces without effects of sample local density of states [19]. Atomically resolved STM images showed an oxygen contamination below 1%.

3. Results and discussions

STM topographic images obtained on the bcc-Fe $\{110\}$ surface shows several terraces with a step height of 0.21 ± 0.03 nm, which is consistent with the bcc-Fe $\{110\}$ plane thickness of $\sqrt{2}a/2 \approx 0.203$ nm, where $a = 0.287$ nm is the lattice constant in the conventional bcc unit cell of α -Fe. We observed a regular array of bright patches of 4 nm in diameter on a single terrace of an Fe $\{110\}$ crystallographic plane in topographic images as shown in Fig. 2a. Fourier transform of this pattern is shown in the inset of Fig. 2a, which indicates that the pattern is aligned nearly along the $[\bar{1}11]$, $[001]$ and $[1\bar{1}\bar{1}]$ directions on Fe $\{110\}$. Note that the bcc- $\{110\}$ planes do not have hexagonal symmetry, but they have only two-fold symmetry.

The pattern was observed on the $\{110\}$ side planes of three different hexagonal-pillar shaped Fe-whiskers. This implies that the

pattern comes from a surface reconstruction intrinsic to the $\{110\}$ planes of bcc-Fe. The same topographic image in higher resolution (14×14 nm²) is shown in Fig. 2b, where not only the pattern but also atomic arrangement can be observed. The height variation along the broken arrow in Fig. 2b is shown in Fig. 2c. The height of the pattern is roughly $0.07 \sim 0.08$ nm, about 1/3 of the step height. The periodicity is about 14 atomic spacings. A two-dimensional Fourier transformed image of Fig. 2b is shown in Fig. 2d. The elements inside the solid circle in the center of the image indicate the same symmetry as the inset of Fig. 2a. White dots inside the six dotted-circles apart from the center show the symmetry of the surface atomic arrangement. Solid and dotted lines show a perfect hexagonal symmetry and a bcc- $\{110\}$ symmetry, respectively. Positions of the six dotted-circles almost fit to the hexagonal symmetry (solid lines) but not to the bcc- $\{110\}$ symmetry, which indicates that the surface atoms do not have a bcc- $\{110\}$ symmetry, but they have almost hexagonal symmetry in spite of the fact that the X-ray measurements in Fig. 1 showed bcc- $\{110\}$. These six dotted-circles are arranged at every $61.5 \pm 2.5^\circ$ and the distances from the center of the image to the six dotted-circles are not exact constant ($\pm 3\%$). These experimental results show that the top surface layer of the bcc Fe $\{110\}$ -whisker has a quasi-hexagonal two-dimensional lattice plane. This will be the essential idea for our interpretation of the experimentally observed surface reconstruction of the Fe $\{110\}$ surface.

An inverse Fourier transformation with elements inside the six dotted-circles and the center circle in the Fourier transformed image (Fig. 2d) give an image shown in Fig. 2e, which shows a clear periodicity of the patterned modulation in brightness as well as the atomic array in the top-layer. From this image, we can get the unit vectors of the height modulation pattern as

$$\begin{pmatrix} \vec{p}_1 \\ \vec{p}_2 \end{pmatrix} = \begin{pmatrix} 13 & 1 \\ -2 & 14 \end{pmatrix} \begin{pmatrix} \vec{u}_1 \\ \vec{u}_2 \end{pmatrix}, \quad (1)$$

where \vec{u}_1 and \vec{u}_2 denote primitive vectors of the atomic arrangement in the top-layer. We set a whisker crystal on our STM stage as shown in Fig. 2a, i.e. the direction of one of the unit vectors of periodic modulation, \vec{p}_1 , was set in almost $[001]$ crystalline direction. The length of \vec{p}_1 was observed to be about 3.65 nm in Fig. 2e, i.e. $|\vec{p}_1|/a \approx 12.7$. Angle between \vec{p}_1 and another unit vector of \vec{p}_2 is $\phi_p \approx 63.8^\circ$, and $k = |\vec{p}_2|/|\vec{p}_1| \approx 0.920$, i.e. $|\vec{p}_2|/a \approx 11.7$.

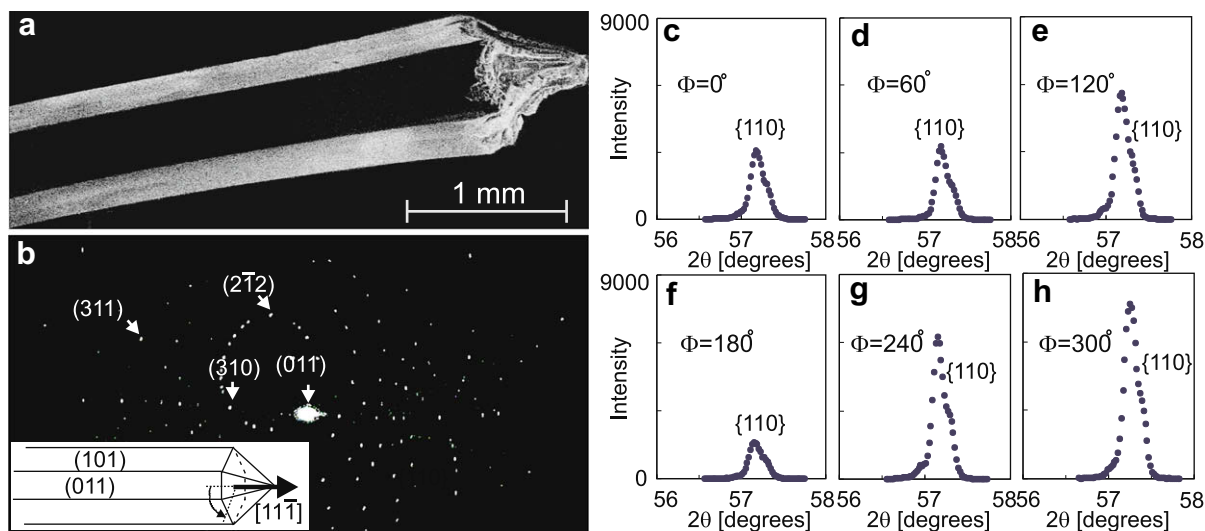


Fig. 1. (a) Scanning electron microscopy image of an Fe-whisker in hexagonal-pillar shape. (b) Laue X-ray image obtained on a side plane of the whisker in (a). An inset sketch shows the crystalline structure of the whisker. (c–h) Diffraction spectra were measured by rotating the whisker at $\Phi = 0^\circ$ (c), 60° (d), 120° (e), 180° (f), 240° (g), and 300° (h). Six side planes of the hexagonal Fe-whisker were identified to be $\{110\}$ using a four circle X-ray diffract meter.

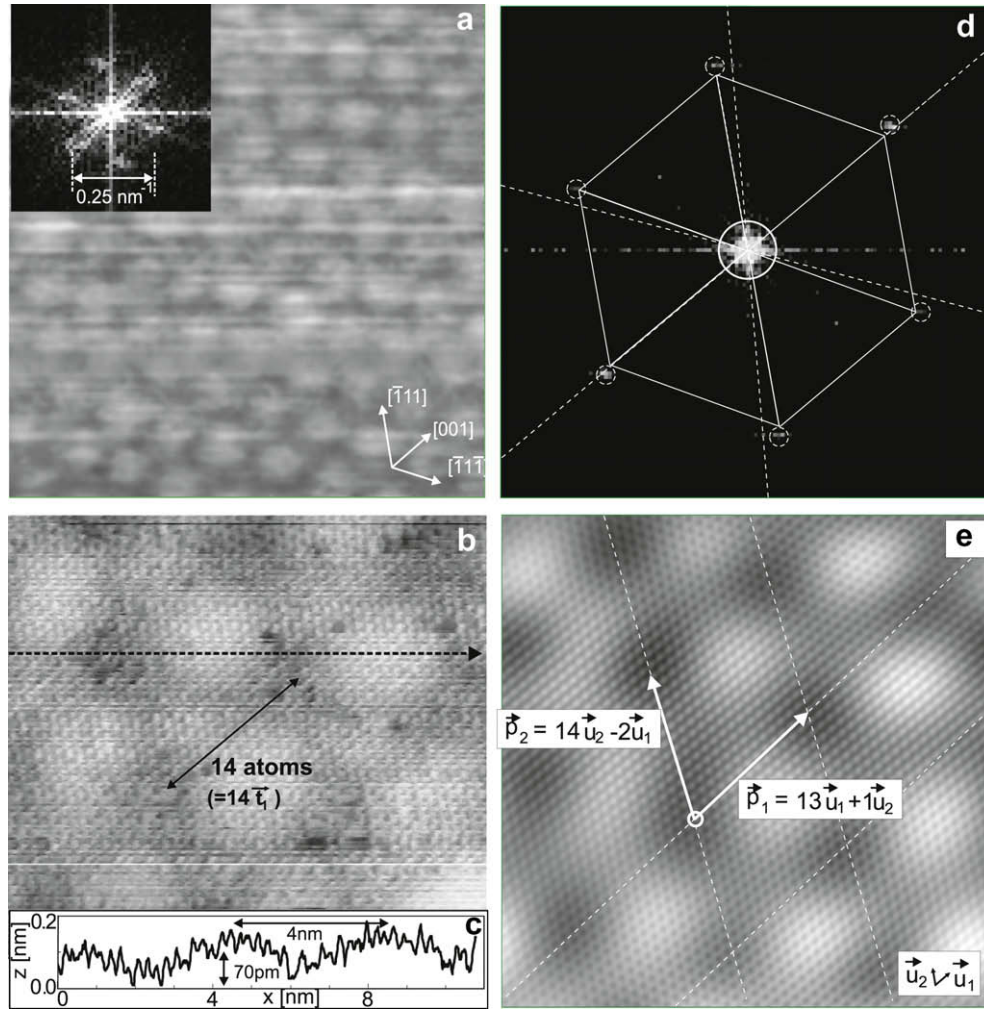


Fig. 2. (a) An STM image obtained on the bcc- α -Fe(110) surface ($34 \times 34 \text{ nm}^2$). The inset image in (a) denotes a Fourier transformed image of (a). (b) An atomically resolved STM image of the {110} surface. The pattern array as well as the atomic array is observed. (c) A line profile along the broken arrow in (b). (d) A Fourier transformed image of (b). (e) An inverse Fourier transformation of (d).

The surface reconstruction pattern is formed by a superposition of a two-dimensional quasi-hexagonal atomic array of the top-layer and the sub-surface bcc- $\{110\}$, which is simply interpreted using a solid-sphere model in Fig. 3. Surface-atoms in the center of the darker areas in the STM-topographic images in Fig. 2 are considered to sit just on the hollow sites of the sub-surface bcc- $\{110\}$ layer, what we cannot see in STM. Let us take unit vectors \hat{x} and \hat{y} along the $[001]$ and $[1\bar{1}0]$ directions on the $\{110\}$ sub-surface of bcc-Fe. Using a lattice constant $a = 0.287 \text{ nm}$, primitive vectors of \vec{s}_1 and \vec{s}_2 in the two-dimensional $\{110\}$ sub-surface plane are expressed as, $\begin{pmatrix} \vec{s}_1 \\ \vec{s}_2 \end{pmatrix} = a \begin{pmatrix} 1 & 0 \\ 1/2 & 1/\sqrt{2} \end{pmatrix} \begin{pmatrix} \hat{x} \\ \hat{y} \end{pmatrix}$. A solid-sphere model of the sub-surface bcc-Fe $\{110\}$ is shown in Fig. 3a, where hollow sites are indicated by black dots, what makes a triangular lattice with two-fold symmetry different from the quasi-hexagonal lattice of atomic sites in the top-layer.

Since the observed height modulation pattern appears as the interference between the atomic array of the top-layer and the hollow sites on the sub-surface layer, the unit vectors of the modulation, $\vec{p}_j (j = 1, 2)$, must also be expressed by the primitive vectors $\vec{s}_j (j = 1, 2)$, of the hollow sites on the sub-surface layer, i.e.,

$$\begin{pmatrix} \vec{p}_1 \\ \vec{p}_2 \end{pmatrix} = \begin{pmatrix} m_1 & n_1 \\ m_2 & n_2 \end{pmatrix} \begin{pmatrix} \vec{s}_1 \\ \vec{s}_2 \end{pmatrix} = a \begin{pmatrix} m_1 + n_1/2 & n_1/\sqrt{2} \\ m_2 + n_2/2 & n_2/\sqrt{2} \end{pmatrix} \begin{pmatrix} \hat{x} \\ \hat{y} \end{pmatrix}, \quad (2)$$

where m_1, n_1, m_2 , and n_2 are integers, which determine \vec{p}_1 and \vec{p}_2 exactly. Angles between $\vec{p}_j (j = 1, 2)$ and the $[001](\hat{x})$ direction are given by $\phi_j = \arctan(\sqrt{2}n_j/(2m_j + n_j))$, ($j = 1, 2$).

If a correct set of integers, m_1, n_1, m_2 , and n_2 , are obtained, \vec{p}_j and also \vec{u}_j are related to \vec{s}_j which is strictly defined by the lattice constant due to constrain of bcc structure in three dimensions. Quantitatively precise results, which improve upon the direct STM image, can be obtained. First, we put n_1 as an integer near zero (e.g. $0, \pm 1, \dots, \pm 5$ in Table 1) since the sample is mounted with ϕ_1 not far from zero. Then, an integer m_1 is selected to give a minimum deviation, $\Delta_1 = \|\vec{p}_1^{\text{exp}}\|/a - \|\vec{p}_1^{\text{cal}}\|/a$, where $\|\vec{p}_1^{\text{exp}}\|/a$ denotes the experimentally obtained $\|\vec{p}_1\|/a \approx 12.7$, and $\|\vec{p}_1^{\text{cal}}\|/a = \sqrt{(m_1 + n_1/2)^2 + n_1^2/2}$. Integers n_2 and m_2 are determined so as to give a minimum deviation in components of $\|\vec{p}_2^{\text{exp}}\|/a$, $\Delta_y = |(\|\vec{p}_2^{\text{exp}}\|/a) \sin(\phi_1 + \phi_p) - n_2/\sqrt{2}|$, $\Delta_x = |(\|\vec{p}_2^{\text{exp}}\|/a) \cos(\phi_1 + \phi_p) - (n_2/2 + m_2)|$, where $\|\vec{p}_2^{\text{exp}}\|/a$ denotes the experimentally obtained $\|\vec{p}_2\|/a \approx 11.7$, and $\phi_p \approx 63.8^\circ$. The total deviation $\Delta = \sqrt{\Delta_1^2 + \Delta_y^2 + \Delta_x^2}$ can be useful to judge the most reasonable set of n_1, m_1, n_2 , and m_2 . Table 1 shows several sets of candidate integers. Each set gives different $\phi_j (j = 1, 2)$. In these sets, the most reasonable relation with the minimum total deviation is

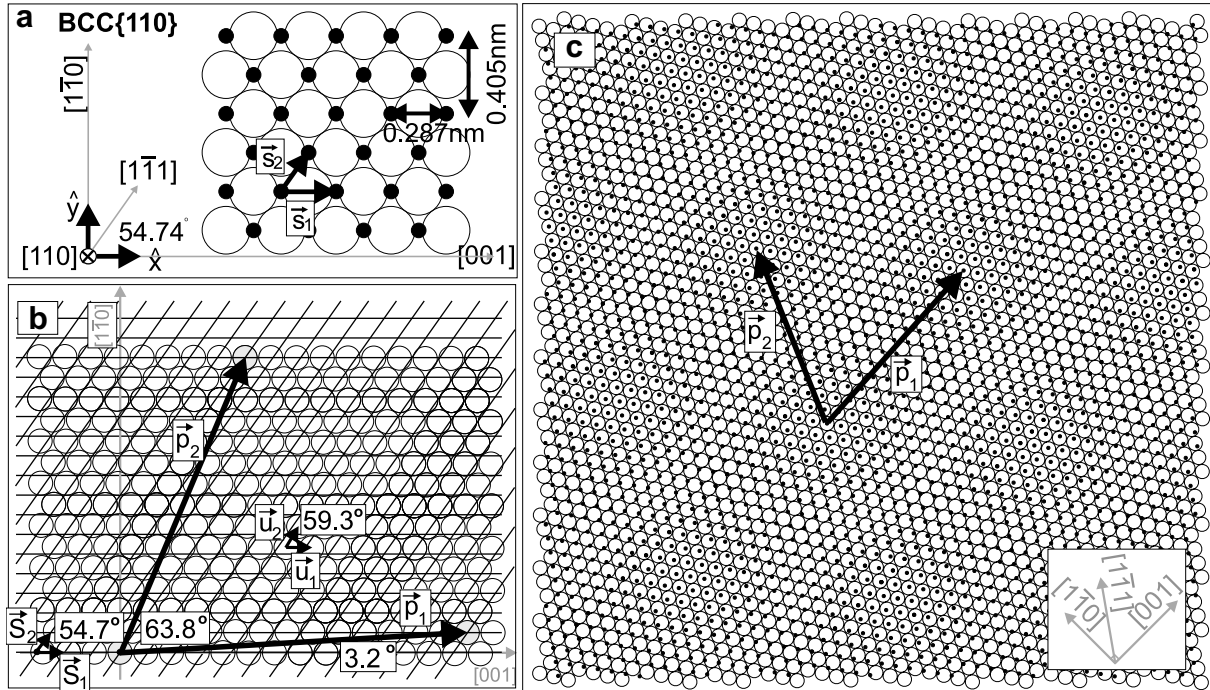


Fig. 3. Solid-sphere models on the surface of α -Fe(110). White circles and black dots show Fe atoms and hollow sites, respectively. (a) A conventional bcc- α -Fe(110) lattice plane. \vec{s}_1 and \vec{s}_2 are primitive vectors. (b) Relations of the primitive vectors of the quasi-hexagonal top-layer (\vec{u}_1 and \vec{u}_2), the sub-surface (\vec{s}_1 and \vec{s}_2) layer and the modulation pattern (\vec{p}_1 and \vec{p}_2). Lines are parallel to the sub-surface primitive vectors. (c) A superposition of the quasi-hexagonal top-layer lattice plane and the sub-surface conventional bcc-(110).

Table 1

Obtained integers for n_1 , n_2 , m_1 and m_2 . ϕ_j denotes the angle between the [001] direction and \vec{p}_j ($j = 1, 2$). The total deviation is shown as $\Delta = (\Delta_1^2 + \Delta_2^2 + \Delta_3^2)^{0.5}$.

n_1	m_1	n_2	m_2	ϕ_1	ϕ_2	Δ
-5	15	12	2	-16.1	46.7	0.34
-4	14	13	1	-12.8	50.8	0.43
-3	14	13	0	-9.6	54.7	0.43
-2	14	14	-1	-6.4	58.8	0.46
-1	13	14	-1	-3.2	63.2	0.80
0	13	15	-2	0.0	62.6	0.47
1	12	15	-3	3.2	67.0	0.25
2	12	16	-4	6.4	70.5	0.49
3	11	16	-5	9.6	75.1	0.36
4	10	16	-5	12.8	75.1	0.50
5	10	16	-6	16.1	80.0	0.33

$$\begin{pmatrix} \vec{p}_1 \\ \vec{p}_2 \end{pmatrix} = \begin{pmatrix} 12 & 1 \\ -3 & 15 \end{pmatrix} \begin{pmatrix} \vec{s}_1 \\ \vec{s}_2 \end{pmatrix} = a \begin{pmatrix} 12.5 & 1/\sqrt{2} \\ 4.5 & 15/\sqrt{2} \end{pmatrix} \begin{pmatrix} \hat{x} \\ \hat{y} \end{pmatrix} \quad (3)$$

The relation between the top-layer and the sub-surface layer can be deduced from Eqs. (1) and (3) as follows:

$$\begin{pmatrix} \vec{u}_1 \\ \vec{u}_2 \end{pmatrix} = \begin{pmatrix} 13 & 1 \\ -2 & 14 \end{pmatrix}^{-1} \begin{pmatrix} 12 & 1 \\ -3 & 15 \end{pmatrix} \begin{pmatrix} \vec{s}_1 \\ \vec{s}_2 \end{pmatrix} \quad (4)$$

This relation is graphically shown in Fig. 3b, where the two-dimensional lattice of the top-layer is not any longer a perfect hexagonal lattice. The angle between \vec{u}_1 and \vec{u}_2 is 59.3° , and \vec{u}_1 rotates by -0.2° from \vec{s}_1 , i.e. they are nearly parallel though \vec{p}_1 rotates by 3.2 (3.4) $^\circ$ from \vec{s}_1 (\vec{u}_1). Absolute values of primitive vectors are as follows, $|\vec{s}_1| = a > |\vec{u}_1| = 0.927a > |\vec{u}_2| = 0.883a > |\vec{s}_2| = 0.866a$. A model is made with these primitive vectors, where the hollow sites on the sub-surface layer marked as black dots are superposed by surface atoms marked by the white circles. This superposition represents a periodic pattern as shown in Fig. 3c, which is consistent with the obtained STM topographic image of Fig. 2.

According to the solid-sphere contact model, the maximum height difference of the modulation is $\Delta h = (\sqrt{3} - \sqrt{2})a/2 \approx 0.046$ nm. The experimentally obtained STM images at negative bias voltages show the height difference of 0.07–0.08 nm, which is somewhat larger than the value suggested by the solid-sphere contact model. Since the tunneling currents, i.e. STM images, obtained at negative bias voltages are not strongly influenced by sample electronic states [19], this height difference of 0.07–0.08 nm can be considered as a real height difference. Then, the larger different height may have physical meaning. Since the radius of the solid-sphere in the solid-sphere model is estimated for an atom surrounded by eight nearest neighbors in the bulk bcc-Fe, the model does not include influences of the different symmetries, i.e. coordination numbers, of the surface atoms. In the top surface layer, atoms on the hollow sites have a higher coordination number than the atoms on the atomic sites. Therefore, an experimentally obtained height difference larger than the model expects indicates an atomic distance larger than the distance in bulk for the atoms on the atomic sites, which can be also explained by the fact that the NN distance in bulk is shorter than the potential minimum distance between two atoms, i.e. atoms with a lower coordination number prefer to take a larger atomic distance.

Two-dimensional density of atoms in the sub-surface bcc-{110} is $1/|\vec{s}_1 \times \vec{s}_2| = \sqrt{2}/a^2$, while that in the top surface layer is $1/|\vec{u}_1 \times \vec{u}_2| = 1.0046/|\vec{s}_1 \times \vec{s}_2|$. This slight difference of less than 0.5% is within errors in direct experimental observation, however, in our procedure of analysis it can be meaningful. This fact that a surface of condensed matter has higher density of atoms than a bulk due to the so-called surface tension, which is caused by the break down in symmetry of interactions between the atoms.

The observed height difference between dark and bright regions in the STM image of top-layer is larger than that expected from the simple hard-contact solid-sphere model. The number of atoms in a unit cell of the periodic pattern of the height modulation in

the flat sub-surface bcc-{1 1 0} layer is $|\vec{p}_1 \times \vec{p}_2| / |\vec{s}_1 \times \vec{s}_2| = 91.50$, while that in the top-layer is $|\vec{p}_1 \times \vec{p}_2| / |\vec{u}_1 \times \vec{u}_2| = 91.92$. This slight excess number of atoms is accommodated in bright concave regions in the non-flat top-layer.

There may be another possibility to cause the reconstruction on the Fe{1 1 0}. Although our Auger spectroscopy and atomically resolved STM images detected only oxygen atoms with a concentration below 1%, these techniques cannot detect hydrogen. Theoretical calculations and low-energy electron diffraction results showed a hydrogen-induced (2×2) reconstruction on the Fe{1 1 0} surface at low temperatures (~ 40 K) by introducing hydrogen gas under the base pressure in a range of 10^{-8} – 10^{-9} Pa [20,21], a pressure that is comparable to our experimental setup. (The Fe single crystal used in Ref. [21] includes impurities of S, P, C in bulk.) So far, hydrogen-induced (2×2) reconstruction was found only below 300 K and we did not observe a short-period reconstruction, like (2×2), on our Fe{1 1 0} surface at 300 K. Therefore, we consider that the mesoscopic-range reconstruction that we found on the clean Fe{1 1 0} surface is likely not caused by hydrogen atoms.

4. Conclusion

Clean bcc-{1 1 0} surfaces of three different pure hexagonal-pillar shaped α -Fe-whiskers was investigated by means of STM at RT in UHV. The top surface layer was found to be reconstructed to a quasi-hexagonal atomic array with periodic height modulation. Unit vectors of the modulation turned out to be expressed as $\begin{pmatrix} \vec{p}_1 \\ \vec{p}_2 \end{pmatrix} = \begin{pmatrix} 13 & 1 \\ -2 & 14 \end{pmatrix} \begin{pmatrix} \vec{u}_1 \\ \vec{u}_2 \end{pmatrix} = \begin{pmatrix} 12 & 1 \\ -3 & 15 \end{pmatrix} \begin{pmatrix} \vec{s}_1 \\ \vec{s}_2 \end{pmatrix}$, where $\begin{pmatrix} \vec{u}_1 \\ \vec{u}_2 \end{pmatrix}$ and $\begin{pmatrix} \vec{s}_1 \\ \vec{s}_2 \end{pmatrix}$ are the primitive vectors of the two-dimensional atomic array in the top-layer and those in the sub-surface layer, respectively. The two-dimensional density of atoms in the top-layer is slightly higher by 0.46% than that in the sub-surface layer.

Acknowledgements

We would like to appreciate to Prof. Dr. W. Wulfhekel, Prof. Dr. H. van Kempen and Prof. Dr. F. Spaepen for helpful discussions. Kind guidance for CVD for Fe-whisker by Dr. D.T. Pierce is acknowledged.

References

- [1] H. Hasegawa, D.G. Pettifor, Phys. Rev. Lett. 50 (1983) 130.
- [2] G.L. Krasko, G.B. Olson, Phys. Rev. B 40 (1989) 11536.
- [3] M.A. van Hove, R.J. Koestner, P.C. Stair, J.P. Bibérian, L.L. Kesmodel, I. Bartos, G.A. Somorjai, Surf. Sci. 103 (1981) 189; M.A. van Hove, R.J. Koestner, P.C. Stair, J.P. Bibérian, L.L. Kesmodel, I. Bartos, G.A. Somorjai, Surf. Sci. 103 (1981) 218.
- [4] R.T. Tung, W.R. Graham, A.J. Melmed, Surf. Sci. 115 (1982) 576.
- [5] P.R. Norton, J.A. Davies, D.K. Creber, C.W. Sitter, T.E. Jackman, Surf. Sci. 108 (1981) 205.
- [6] P. Fery, W. Moritz, D. Wolf, Phys. Rev. B 38 (1988) 7275.
- [7] J. Weissenrieder, M. Göthelid, M. Mansson, H. von Schenck, O. Tjernberg, U.O. Karlsson, Surf. Sci. 527 (2003) 163.
- [8] J. Weissenrieder, M. Göthelid, G.L. Kay, U.O. Karlsson, Surf. Sci. 515 (2002) 135.
- [9] J.A. Stroscio, D.T. Pierce, Phys. Rev. B 49 (1994) 8522.
- [10] R.J. Schäfer, R. Urban, D. Ullmann, H.L. Meyerheim, B. Heinrich, L. Schultz, J. Kirschner, Phys. Rev. B 65 (2002) 144405.
- [11] J.A. Stroscio, D.T. Pierce, A. Davies, R.J. Celotta, M. Weinert, Phys. Rev. Lett. 75 (1995) 2960.
- [12] M.M.J. Bischoff, T.K. Yamada, C.M. Fang, R.A. de Groot, H. van Kempen, Phys. Rev. B 68 (2003) 045422.
- [13] S.T. Purcell, A.S. Arrott, B. Heinrich, J. Vac. Sci. Technol. B 6 (1988) 794.
- [14] A. Biedermann, W. Rupp, M. Schmid, P. Varga, Phys. Rev. B 73 (2006) 165418.
- [15] A. Biedermann, R. Tscheliessnig, M. Schmid, P. Varga, Phys. Rev. Lett. 87 (2001) 086103.
- [16] V. Blum, Ch. Rath, S. Muller, L. Hammer, K. Heinz, J.M. Garcia, J.E. Ortega, J.E. Prieto, O.S. Herman, J.M. Gallego, A.L. Vazquez de Parga, R. Miranda, Phys. Rev. B 59 (1999) 15966.
- [17] M. Bode, R. Pascal, M. Dreyer, R. Wiesendanger, Phys. Rev. B 54 (1996) R8385.
- [18] D.M. Gillingham, M. Tselepi, A. Ionescu, S.J. Steinmuller, H.E. Beere, D.A. Ritchie, J.A.C. Bland, Phys. Rev. B 76 (2007) 214412.
- [19] V.A. Ukraintsev, Phys. Rev. B 53 (1996) 11176.
- [20] D.E. Jiang, E.A. Carter, Surf. Sci. 547 (2003) 85.
- [21] L. Hammer, H. Landskron, W. Nichtl-Pecher, A. Fricke, K. Heinz, K. Müller, Phys. Rev. B 47 (1993) 15969.